

Isotopic effects in (surface enhanced) Raman spectroscopy – Single molecule aspects

Stephan Kupfer¹, Volker Deckert^{1,2} and Stefanie Gräfe¹

¹*Institute of Physical Chemistry and Abbe Center of Photonics, Friedrich-Schiller-University Jena, Helmholtzweg 4, 07743 Jena, Germany*

²*Institute of Photonic Technology Jena (IPHT), Albert-Einstein-Straße 9, 07745 Jena, Germany*

Dedicated to Professor Wolfgang Kiefer on the occasion of his 75th birthday

Generally, isotopic effects are of minor importance in standard vibrational spectroscopy, this is in particular the case, if the signal originates from a macroscopic sample. Consequently, an average spectrum with respect to the natural isotopic redundancy is obtained. However, for *State-of-the-Art* high-resolution techniques, e.g. surface-enhanced Raman spectroscopy, where only a small number of molecules (or even merely a single molecule) are the focus of the exciting beam, isotopic effects can have a considerable influence on the spectral pattern. Here we present a computational study investigating such isotopic effects on the Raman spectrum for the ¹³C isotope in the thiophenol molecule. Therefore, the Raman spectra of all four possible singly ¹³C doped species are calculated at the density functional theory level of theory and compared to the undoped thiophenol reference spectrum. The impact of ¹³C substitution on the vibrational frequencies as well as on the Raman intensities is rationalized. In particular large effects are determined for the in-plane vibrational modes, while each of the five calculated species (one undoped and 4 singly doped) features a unique Raman intensity pattern. © Anita Publications. All rights reserved.

Keywords: Isotopic effects, Laser pulses, Thiophenol, Surface-enhanced Raman spectroscopy (SERS)

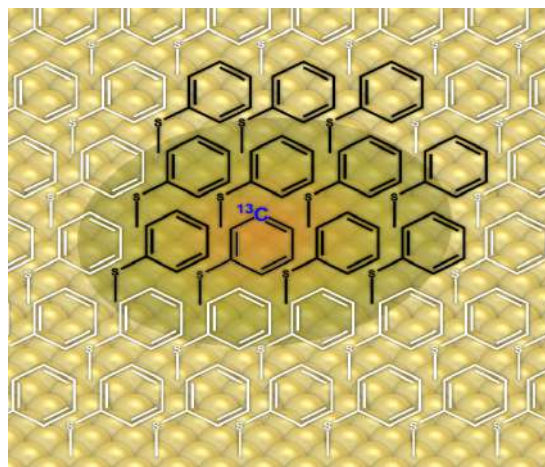
1 Introduction

In optical spectroscopy isotope effects are well known and often used in a directed way to obtain specific information about chemical bonds, structural conformations and chemical reactivity in general. Apart from those specific applications the isotopic ratios can be considered as constant, at least when working with natural abundant material. This is particularly true for organic substances as the natural abundance of the main constituents namely hydrogen and carbon. While it is clear, that mass isotopes result in a shift of spectroscopic bands, in optical spectroscopy this effect can be disregarded because the ratio of the isotopes is constant. As the specific site of the isotopic label in a natural compound or a compound synthesized with a natural isotope abundance must vary statistically, disregarding those effects can be only justified as long as the number of investigated molecules is large compared to the labeling sites. This condition is generally easily fulfilled in a spectroscopic experiment. Even in a microscope focus one finds roughly 10^{10} molecules and proper averaging can be safely assumed. Recent developments in technology, however, allow for a much higher spatial resolution even down to single molecule sensitivity. Prominent examples are single molecule surface enhanced Raman spectroscopy [1-4] (SERS) where specific hot spots are considered to play an important role or tip-enhanced Raman spectroscopy [5-7] where also hot spots are involved, however, in a very directed way. In such cases a statistical averaging cannot be expected anymore. Consequently, the spectra will show intrinsic features due to a specific isotopic labeling. In contrast to the above mentioned

Corresponding author :

e-mail: volker.deckert@uni-jena.de; phone: 49-3641-948347 (Volker Deckert);
s.graefe@uni-jena.de; phone: 49-3641-948330 (Stefanie Gräfe)

“controlled” experiments the labeling is statistically distributed over all atoms of the molecule and uniform spectra cannot be expected. While this effect is a direct consequence of the natural abundance of isotopes it is an unfamiliar concept in spectroscopy to have different band positions and intensities for the “same” chemical structure even without considering specific molecular orientations. We will discuss specifically the effect of ^{13}C labeling on a thiophenol. As a relatively simple molecule the number of distinct positions are limited, further it was already extensively studied by SERS and more importantly this molecule forms self-assembled monolayers,[8-12] see Fig 1, that provide a basis for dedicated experiments to also experimentally investigate such effects in addition to the theoretical investigation presented here.



F

Fig 1. SERS setup with thiophenol anchored on Gold surface, molecules excited by laser beam in black with the ^{13}C doped Carbon atom in blue.

From a computational point of view several studies investigated isotopic effects in chemical reactions, i.e. thermodynamic and kinetic properties with respect to transition states [1,13-15] as well as the kinetic isotopic effect in competitive $\text{S}_{\text{N}}2$ (bimolecular nucleophilic substitution) and E_2 (bimolecular elimination) reaction pathways [16-19]. Further combined experimental-theoretical studies focused on isotopic effects in vibrational spectroscopy, while density functional theory (DFT) proved to yield good agreements with respect to experimentally observed frequency shifts [20-24]. However, much less is known concerning the influence of isotopic effects on intensities in vibrational spectroscopy, in particular with respect to Raman spectroscopy [25].

Here we present a combined experimental-theoretical investigation on the influence of ^{13}C on the Raman spectrum of thiophenol. Therefore, DFT calculations are applied to determine effects on the vibrational frequencies as well as on the Raman intensities.

2 Computational Details

All quantum chemical calculations were performed using the program package Gaussian 09 [26]. The fully optimized equilibrium structure of thiophenol was obtained at the DFT level of theory by means of the B3LYP [27,28] XC functional and the 6-31G(d) double- ζ basis set [29] in gas phase. A subsequently performed vibrational analysis yielded the vibrational normal modes, frequencies and Raman activities. Gaussian 09 uses by default the mass of the most abundant isotopes that is ^1H with 1.00783 amu for Hydrogen, ^{12}C with 12.00000 amu for Carbon and ^{32}S with 31.97207 amu for Sulphur [30,31]. In order to investigate

the impact of isotopic effects on the Raman pattern, further vibrational calculations were performed by substituting a single ^{12}C atom with ^{13}C . This was done for the Carbon atoms C1-C4 as depicted in Fig 2.

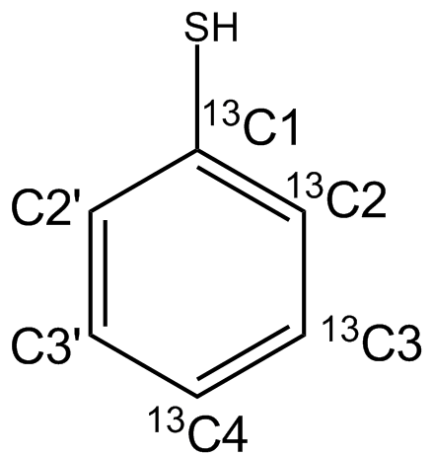


Fig 2. Molecular structure of thiophenol with labeled single ^{13}C substitution sites that is $^{13}\text{C1}$ at the thiol group, in *ortho* $^{13}\text{C2}$, *meta* $^{13}\text{C3}$ and in *para* position $^{13}\text{C4}$.

Based on the natural abundances of the Carbon isotopes of approximately 98.93% ^{12}C and 1.07% ^{13}C [32], the proportions of the singly doped thiophenol species are 0.18% C1, 0.36% C2, 0.36% C3 and 0.18% C4. The vibrational frequencies of the undoped thiophenol (^{12}C only) and of the four single doped forms (^{12}C only) were scaled by a factor of 0.97 in order to correct for the lack of anharmonicity and the approximate treatment of electron correlation; the vibrational modes were broadened by Lorentzian functions with a full-width at half maximum of 20 cm^{-1} to generate a typical Raman band structure.

3 Results and Discussion

The ground state structure of thiophenol optimized at the B3LYP/6-31G(d) level of theory is of C_s symmetry, thus, the SH fragment is oriented perpendicular to the aromatic plane of the phenyl fragment. Carbon-Carbon bond lengths of 1.3996 Å for C1-C2 and 1.3960 Å for C2-C3 and C3-C4 are obtained, while for the Carbon-Sulphur bond a value of 1.8068 Å is found (see Fig 2). For the Carbon-Hydrogen bond lengths values of 1.0857, 1.0868 and 1.0687 Å are obtained in *ortho*-, *meta*- and *para*-position, respectively, while the Sulphur-Hydrogen bond features an equilibrium length of 1.3530 Å. The phenyl moiety is almost perfectly planar as rationalized by means of the dihedral angle spanned by the Carbon atoms C2-C3-C3'-C2' of 0.01° . However, the Sulphur atom is slightly displaced with respect to the aromatic plane, which is evident from the C4-C1-S angle of 178.20° .

The focus of the vibrational analysis is set on the vibrational normal modes that feature the most pronounced impact on the Raman intensity pattern with respect to single ^{13}C substitution, thus, the further discussion is confined to the frequency range between 500 and 1700 cm^{-1} represented by the vibrational modes 7 to 27. The thiophenol Raman spectrum obtained for the natural isotope redundancy of Carbon that is 98.93% ^{12}C and 1.07% ^{13}C , depicted in Fig (3a). Therefore, such spectrum is correlated to a macroscopic average of Raman signals originating from the collective amount of undoped and doped thiophenol species (in different orientations). Thus, it is obtained by summation over the Raman signals of the five species (see Fig 3b) weighted by the respective probability.

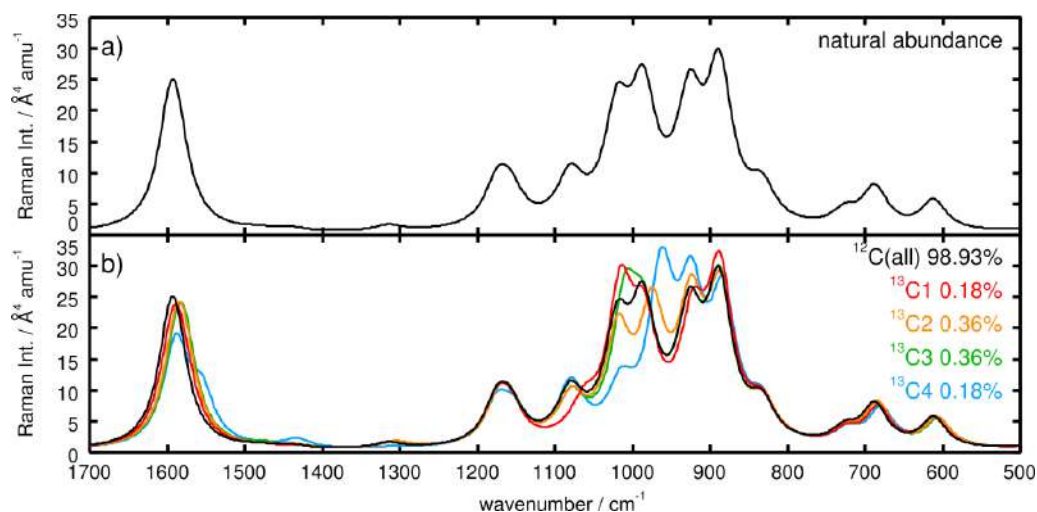


Fig 3. Simulated Raman spectrum obtained for, (a), the natural Carbon isotope abundance (98.93% ^{12}C and 1.07% ^{13}C) and, (b), the undoped thiophenol (in black) and the single doped ^{13}C spectra $^{13}\text{C}1$ (red), $^{13}\text{C}2$ (orange), $^{13}\text{C}3$ (green) and $^{13}\text{C}4$ (blue).

These species are the undoped form with exclusively ^{12}C , and the four singly doped forms $^{13}\text{C}1$ - $^{13}\text{C}4$, while $^{13}\text{C}2$ and $^{13}\text{C}3$ feature the double weight (0.36%) with respect to $^{13}\text{C}1$ and $^{13}\text{C}4$ (0.18%) due to the C_s symmetry of thiophenol.

The Raman spectrum of the undoped thiophenol ($^{12}\text{C}(\text{all})$ in Fig (3b)) features weak bands and shoulders at approximately 723, 834, 1314 and 1446 cm^{-1} , medium intense Raman features at 612, 688, 1078 and 1167 cm^{-1} and intense bands at 890, 924, 988, 1016 and 1592 cm^{-1} . The respective spectra obtained for the single doped form, see $^{13}\text{C}1$, $^{13}\text{C}2$, $^{13}\text{C}3$ and $^{13}\text{C}4$ in Fig (3b), feature partially considerable deviations from the undoped Raman spectrum. Predominate alterations are found in the spectral range between 800 and 1100 cm^{-1} as well as for the band structure at approximately 1600 cm^{-1} . The spectrum of $^{13}\text{C}1$ shows merely slight changes in the position of the intense bands (889, 919, 991, 1013 and 1589 cm^{-1}), however, the band at 1013 cm^{-1} holds an increased intensity. Similar alterations are observed for $^{13}\text{C}2$ with intense bands at 889, 923, 974, 1017 and 1584 cm^{-1} . Opposed to single ^{13}C doping in C1, the Raman band at 1017 cm^{-1} features a decreased intensity with respect to the reference spectrum of the undoped thiophenol. The intensity pattern of $^{13}\text{C}3$ (see Fig (3b)) resembles the pattern of $^{13}\text{C}1$. Here the intense bands are located at 890, 924, 990, 1005 and 1584 cm^{-1} , while the intensity of the band at 1005 cm^{-1} is once more increased with respect to the ^{12}C reference spectrum.

Summation over the five spectra in Fig (3b) namely the undoped ^{12}C spectrum, $^{12}\text{C}(\text{all})$, and the singly doped spectra $^{13}\text{C}1$, $^{13}\text{C}2$, $^{13}\text{C}3$ and $^{13}\text{C}4$ weighted by the factors of 0.9893, 0.0018, 0.0036, 0.0036 and 0.0018, respectively, yields the natural abundance spectrum displayed in Fig (3a). This averaged Raman spectrum is almost identical to the $^{12}\text{C}(\text{all})$ spectrum of Fig (3b), with the five intense bands being found at 890, 924, 988, 1016 and 1592 cm^{-1} . This way it is evident that isotopic effects originating by ^{13}C have no influence on the Raman spectrum on a macroscopic scale.

However, for *State-of-the-Art* spectroscopic techniques that are able to go below the diffraction limit postulated by Ernst Abbe, isotopic effects (e.g. by means of ^{13}C) are of increased significance. This is clearly the case for techniques, where only few or even only a single molecule is in the focus of the laser beam, see Fig 1. In such cases the obtained (Raman) spectrum is no longer an average of a manifold of molecular

orientations and isotopic redundancy. For thiophenol with six Carbon atoms, each Carbon atom is with a probability of 1.07% the ^{13}C isotope; in consequence, the probability to have one ^{13}C atom in thiophenol is 6.42%. Therefore, roughly every 16th thiophene molecule exhibits a ^{13}C atom. In order to investigate the impact of single ^{13}C doping in more detail, the single vibrational modes 7-27 within the spectral range of 500 and 1700 cm^{-1} are studied in more details. The individual Raman spectra of the undoped and the single doped species are depicted in Fig 4(a-e). The vibrational modes of all species are assigned with respect to the modes of the undoped thiophenol ($^{12}\text{C}(\text{all})$), however, the order of the vibrational modes may change upon ^{13}C doping.

The vibrational (Raman active) modes underlying the Raman features of $^{12}\text{C}(\text{all})$ in Fig (3b) at 612, 688, 723, 834, 890, 924, 988, 1016, 1078, 1167, 1314, 1446 and 1592 cm^{-1} are assigned in Fig (4a). The medium bright bands at 612 and 688 cm^{-1} as well as the shoulder at 723 cm^{-1} are correlated to the vibrational modes **7**, **9** and **10** at 611.7, 688.4 and 726.7 cm^{-1} , furthermore the low intensity mode **8** is found at 682.9 cm^{-1} . The band structure between 800 and 1200 cm^{-1} holds contributions from the modes **11-21**, while the shoulders at 834 and 1078 cm^{-1} originate from the modes **11** (1071.4 cm^{-1}) and **19** (1081.0 cm^{-1}), in addition the dark mode **18** is found at 1071.4 cm^{-1} . The vibrational modes **12**, **13**, **16** and **17** at 888.0, 926.5, 986.5 and 1019.9 cm^{-1} contribute to the bands at 890, 924, 988 and 1016, while two further dark modes (**14** and **15**) are localized at 944.7 and 971.8 cm^{-1} , respectively. The modes **20** and **21** (1157.6 and 1174.8 cm^{-1}) contribute to the band at 1167 cm^{-1} .

The frequency range between 1200 and 1500 cm^{-1} shows almost no signal, merely two weak modes at 1314.5 (**23**) and 1441.9 cm^{-1} (**24**) and two dark modes at 1289.1 (**22**) and 1482.1 cm^{-1} (**25**). The Raman band at 1592 cm^{-1} originates from a superposition of two bright modes (**26** and **27**) at 1587.8 and 1594.9 cm^{-1} . Detailed information regarding the displacement vectors or rather the character of the modes **7-27**, frequencies and Raman activities are collected for all five, one undoped and four doped, species in Table 1. Besides, the vibrational frequencies and Raman activities, Table 1 comprises the frequency shifts ($\Delta_{\text{ref}} \tilde{\nu}$ in cm^{-1}) and relative Raman activity deviations of the singly ^{13}C doped species with respect to the undoped ^{12}C reference data. Closer inspection of the spectra shown in Fig (4a-e) and the data in Table 1 reveals that the vibrational frequencies and intensities are partially significantly depending on the ^{13}C substitution pattern.

Evidently only bathochromic shifts of the vibrational frequencies of the doped species are expected with respect to the undoped reference. This follows directly from the increased reduced mass μ_l and the definition of vibrational energy levels ω_{n_l} within the harmonic approximation:

$$\omega_{n_l} = \hbar \sqrt{\frac{k_l}{\mu_l}} (n + 1/2) \quad (1)$$

and the respective transition energy for a fundamental transition from the vibrational ground state (of the electronic ground state) to the first vibrationally excited state:

$$\omega_{0 \rightarrow 1_l} = \hbar \sqrt{\frac{k_l}{\mu_l}} \quad (2)$$

where k_l is the force constant and μ_l the reduced mass for the l th vibrational mode. In accordance, all frequency shifts ($\Delta_{\text{ref}} \tilde{\nu}$) in Table 1 are negative. The most pronounced frequency shifts (see maximum deviations in Table 1) are found for the vibrational modes **16** for $^{13}\text{C}2$, **22** for $^{13}\text{C}1$ and **26** for $^{13}\text{C}3$ and $^{13}\text{C}4$. This phenomenon will be explained exemplarily for the ring breathing mode (**16**), where only very small shifts of -1.2 and 1.1 cm^{-1} are observed for $^{13}\text{C}1$ and $^{13}\text{C}3$ and large shifts of -11.7 and -23.8 cm^{-1} for $^{13}\text{C}2$ and $^{13}\text{C}4$. Taking a closer look into the displacement vector of mode **16** one clearly sees that the Carbon atoms C1 and C3 feature very small displacements, while the atoms C2 and C4 show large displacements.

Thus, an increased reduced mass (^{13}C vs. ^{12}C) has only marginal impact in the positions C1 and C3 on the vibrational frequency and significant influence in C2 and C4. Accordingly, the magnitude of the isotopic effect on all other vibrational modes can be estimated for each ^{13}C position. In general, mainly in-plane vibrational modes, i.e., the modes **16-19** and **22-27** feature substantial shifts. However, the (in-plane) modes **20** and **21** exhibit for all ^{13}C positions only marginal shifts from 0.0 up to merely 4.8 cm^{-1} , this reasoned by means of the small displacements of the Carbon atoms in these modes.

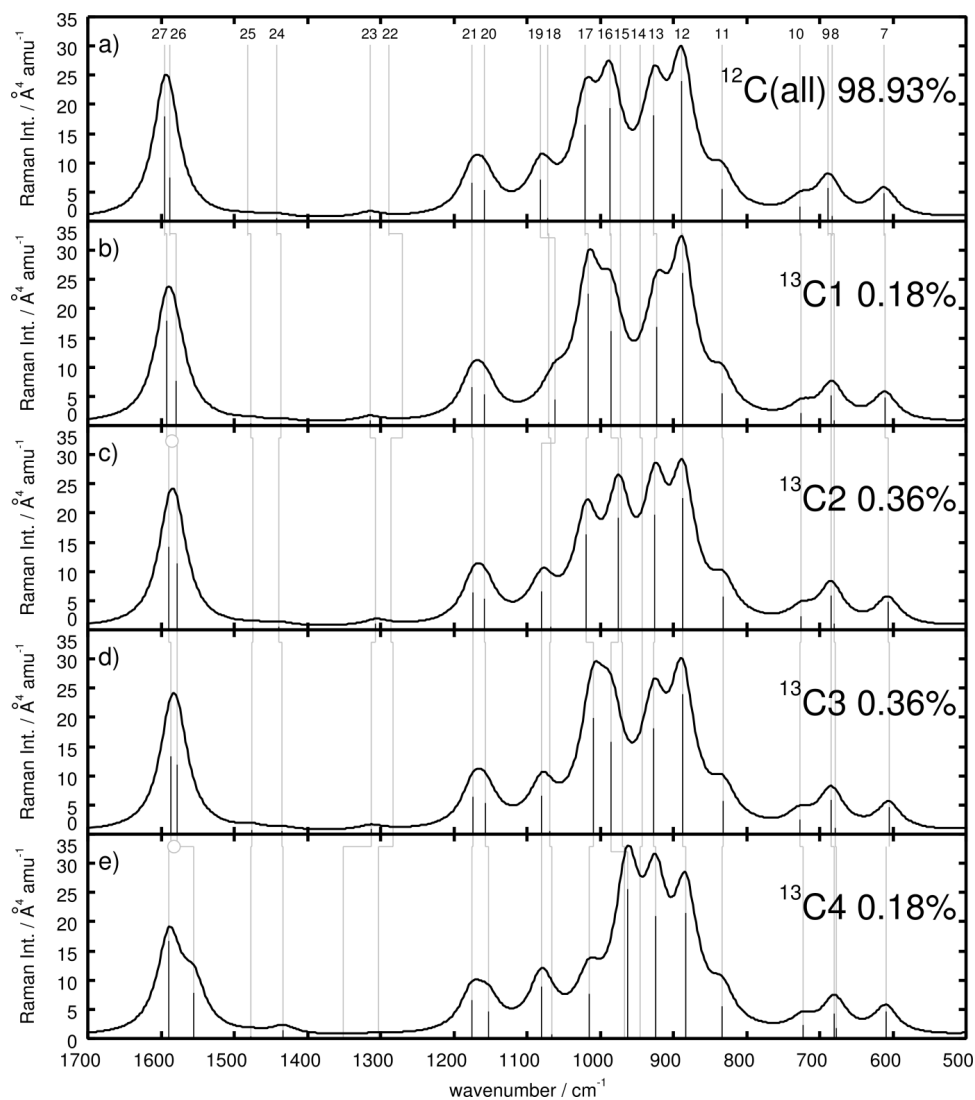
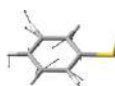
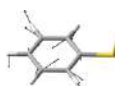







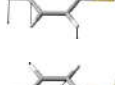

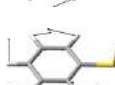





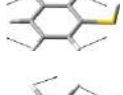
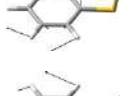
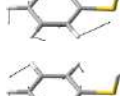
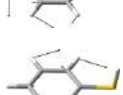

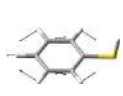
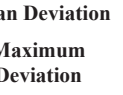
Fig 4. Assignment of the vibrational normal modes for the species, (a), $^{12}\text{C}(\text{all})$, (b), $^{13}\text{C1}$, (c), $^{13}\text{C2}$, (d), $^{13}\text{C3}$ and, (e), $^{13}\text{C4}$. The numbers of the vibrational modes of $^{12}\text{C}(\text{all})$ were used to label the modes of each respective species.

Comparison of the general impact of ^{13}C substitution in C1-C4 is rationalized based on the mean deviations (see [Table 1](#)). The smallest mean deviations are found in the positions C2 and C3 of -3.6 cm^{-1} , a slightly higher value of -4.0 cm^{-1} is observed in C1, while the highest value was found in C4 with -6.0

cm^{-1} . Notably, the induced vibrational shifts lead to alterations in the order of modes, this is in particular the case for the anti-symmetric and the symmetric scissoring modes **18** and **19**, which are inverted for ^{13}C . Also the modes **26** and **27** feature a pronounced mixing for ^{13}C substitution in *ortho*- and *para*- positions.

Table 1. Normal modes (undoped thiophenol) frequencies ($\tilde{\nu}$ in cm^{-1}) and Raman activities (I in $\text{\AA}^4 \text{amu}^{-1}$) for the undoped and the four singly ^{13}C doped species as well as frequency shifts ($\Delta_{\text{ref}} \tilde{\nu}$ in cm^{-1}) and relative Raman activity deviations with respect to the undoped thiophene. Mean deviations and maximum deviations are given for frequency shifts and relative Raman activity deviations

Mode		$\tilde{\nu}/\text{cm}^{-1}$ ($\Delta_{\text{ref}} \tilde{\nu}/\text{cm}^{-1}$)					$I / \text{\AA}^4 \text{amu}^{-1}$ ($I/I_{\text{ref}} - 1$)				
		$^{12}\text{C}(\text{all})$	$^{13}\text{C1}$	$^{13}\text{C2}$	$^{13}\text{C3}$	$^{13}\text{C4}$	$^{12}\text{C}(\text{all})$	$^{13}\text{C1}$	$^{13}\text{C2}$	$^{13}\text{C3}$	$^{13}\text{C4}$
7		611.7 (0.0)	610.7 (-1.0)	606.9 (-4.8)	605.6 (-6.1)	609.8 (-1.9)	4.74 (0.00)	4.75 (0.00)	4.73 (0.00)	4.61 (-0.03)	4.70 (-0.01)
8		682.9 (0.0)	679.6 (-3.3)	680.3 (-2.6)	678.9 (-4.1)	676.9 (-6.0)	0.96 (0.00)	0.93 (-0.03)	1.09 (0.13)	1.01 (0.04)	1.70 (0.76)
9		688.4 (0.0)	683.8 (-4.6)	685.0 (-3.4)	684.7 (-3.6)	680.6 (-7.8)	5.66 (0.00)	5.22 (-0.08)	5.79 (0.02)	5.83 (0.03)	4.31 (-0.24)
10		726.7 (0.0)	724.9 (-1.8)	725.5 (-1.2)	726.6 (-0.1)	723.4 (-3.3)	2.50 (0.00)	2.21 (-0.11)	2.37 (-0.05)	2.50 (0.00)	2.32 (-0.07)
11		833.2 (0.0)	833.2 (0.0)	831.5 (-1.7)	831.5 (-1.7)	833.2 (0.0)	5.55 (0.00)	5.55 (0.00)	5.64 (0.02)	5.66 (0.02)	5.55 (0.00)
12		888.0 (0.0)	887.3 (-0.7)	886.8 (-1.2)	887.9 (-0.1)	883.1 (-4.9)	23.96 (0.00)	26.10 (0.09)	22.52 (-0.06)	24.05 (0.00)	21.55 (-0.10)
13		926.5 (0.0)	922.5 (-4.0)	924.9 (-1.6)	926.4 (-0.1)	924.5 (-2.0)	18.14 (0.00)	16.82 (-0.07)	19.66 (0.08)	18.07 (0.00)	20.99 (0.16)
14		944.7 (0.0)	944.7 (0.0)	942.5 (-2.3)	942.1 (-2.7)	944.7 (0.0)	0.02 (0.00)	0.02 (0.00)	0.11 (5.56)	0.02 (0.05)	0.02 (0.00)
15		971.8 (0.0)	971.8 (0.0)	971.3 (-0.4)	969.9 (-1.9)	967.1 (-4.7)	0.10 (0.00)	0.09 (-0.12)	0.12 (0.17)	0.11 (0.04)	0.06 (-0.40)
16		986.5 (0.0)	985.2 (-1.2)	974.8 (-11.7)	985.3 (-1.1)	962.7 (-23.8)	19.45 (0.00)	16.09 (-0.17)	19.12 (-0.02)	15.83 (-0.19)	25.57 (0.31)
17		1019.9 (0.0)	1015.6 (-4.2)	1018.8 (-1.0)	1009.9 (-10.0)	1015.1 (-4.8)	16.59 (0.00)	22.50 (0.36)	16.37 (-0.01)	19.96 (0.20)	7.70 (-0.54)
18		1071.4 (0.0)	1070.0 (-1.3)	1067.2 (-4.2)	1069.1 (-2.3)	1065.6 (-5.8)	0.59 (0.00)	0.60 (0.03)	0.55 (-0.07)	0.59 (0.01)	0.65 (0.12)

19		1081.0 (0.0)	1061.9 (-19.0)	1079.7 (-1.3)	1079.7 (-1.3)	1080.2 (-0.8)	7.16 (0.00)	4.48 (-0.37)	6.49 (-0.09)	6.53 (-0.09)	8.90 (0.24)
20		1157.6 (0.0)	1157.6 (0.0)	1157.6 (0.0)	1156.5 (-1.2)	1152.9 (-4.8)	5.26 (0.00)	5.26 (0.00)	5.27 (0.00)	5.26 (0.00)	4.66 (-0.11)
21		1174.8 (0.0)	1174.8 (0.0)	1173.1 (-1.7)	1173.4 (-1.4)	1174.8 (0.0)	6.51 (0.00)	6.52 (0.00)	6.35 (-0.02)	6.33 (-0.03)	6.53 (0.00)
22		1289.1 (0.0)	1269.6 (-19.5)	1285.7 (-3.4)	1283.6 (-5.5)	1282.7 (-6.4)	0.01 (0.00)	0.01 (0.44)	0.09 (9.44)	0.05 (4.43)	0.02 (1.31)
23		1314.5 (0.0)	1314.5 (0.0)	1306.5 (-8.0)	1312.8 (-1.7)	1302.7 (-11.8)	0.91 (0.00)	0.91 (0.00)	1.04 (0.14)	0.85 (-0.06)	0.26 (-0.71)
24		1441.9 (0.0)	1435.5 (-6.4)	1438.6 (-3.3)	1434.2 (-7.7)	1433.1 (-8.9)	0.52 (0.00)	0.36 (-0.31)	0.54 (0.05)	0.46 (-0.12)	1.47 (1.82)
25		1482.1 (0.0)	1477.3 (-4.8)	1474.8 (-7.2)	1476.5 (-5.6)	1477.1 (-4.9)	0.37 (0.00)	0.36 (-0.02)	0.28 (-0.23)	0.63 (0.73)	0.32 (-0.11)
26		1587.8 (0.0)	1578.8 (-8.9)	1578.5 (-9.3)	1577.7 (-10.1)	1555.7 (-32.0)	7.51 (0.00)	7.59 (0.01)	11.31 (0.51)	11.91 (0.59)	7.77 (0.03)
27		1594.9 (0.0)	1592.2 (-2.7)	1588.7 (-6.3)	1587.0 (-8.0)	1588.8 (-6.1)	18.00 (0.00)	17.97 (0.00)	14.13 (-0.22)	13.30 (-0.26)	16.69 (-0.07)
	Mean Deviation	0.0	-4.0	-3.6	-3.6	-6.7	0.00	-0.02	0.73	0.26	0.11
	Maximum Deviation	0.0	-19.5	-11.7	-10.1	-32.0	0.00	0.44	9.44	4.43	1.82

Besides the influence of isotopic effects on the vibrational frequencies also considerable alterations with respect to the intensity pattern were calculated. In general the Raman intensity for a fundamental transition (Stokes) is given by:

$$I_{g0 \rightarrow g1_l} = \frac{4e^4}{16\pi^2 \epsilon_0^2 c^4} (\omega_L - \omega_l)^4 |(\alpha_{\alpha,\beta})_{g0 \rightarrow g1_l}|^2 \quad (3)$$

where ω_L is the frequency of the incident light and ω_l the frequency of the l^{th} normal mode. The transition polarizability $(\alpha_{\alpha,\beta})_{g0 \rightarrow g1_l}$ (with its compounds α and β) is universally defined for a transition between any initial state $|i\rangle$ and the final state $|f\rangle$ via the intermediate state $|n\rangle$ as:

$$(\alpha_{\alpha,\beta})_{i \rightarrow f} = \frac{1}{\hbar} \sum_n \left(\frac{\langle f | \hat{\mu}_\alpha | n \rangle \langle n | \hat{\mu}_\beta | i \rangle}{\omega_{n,i} - \omega_L - i\Gamma} + \frac{\langle f | \hat{\mu}_\beta | n \rangle \langle n | \hat{\mu}_\alpha | i \rangle}{\omega_{n,f} + \omega_L + i\Gamma} \right) \quad (4)$$

with the compounds of the dipole operators $\hat{\mu}_\alpha$ and $\hat{\mu}_\beta$ and the damping factor Γ describing homogeneous broadening. The damping factor can be neglected in off-resonant cases since it is small relative to $\omega_{(n,i)}$. As can be seen from Eq (3), the intensity is proportional to $(\omega_L - \omega_l)^4$, thus, an isotopically caused bathochromic shift of the frequency ω_l leads to an increase of its intensity. This is also evident by means of the mean

deviations of the intensity, where only for $^{13}\text{C}1$ a slight decrease (-2%) was observed. For $^{13}\text{C}2$, $^{13}\text{C}3$, and $^{13}\text{C}4$, the intensity increases by 73% , 26% and 11% , respectively. Maximum intensity deviations of 44% ($^{13}\text{C}1$ mode **22**), 944% ($^{13}\text{C}2$ mode **22**), 443% ($^{13}\text{C}3$ mode **22**) and 182% ($^{13}\text{C}4$ mode **24**) are computed, while (allowedly) the highest impact on the intensity was observed for very weakly Raman active modes such as the modes **8**, **14**, **22**, **23**, **24** and **25**. For the very bright modes **12**, **13**, **16** and **17**, moderate variation ranging from -54% to $+36\%$ are found. However, for certain modes the intensity also decreases (e.g. mode **17** with -54%). This is in particular the case for normal modes that show alterations upon substitution with ^{13}C . Examples for such modes are the previously mentioned modes **26** and **27** showing a pronounced mixing in $^{13}\text{C}2$ and $^{13}\text{C}3$, [Table 2](#) displays these modes for all five species. Thus, a direct comparison of the modes and their respective intensities is no longer possible.

Table 2. Vibrational normal modes for $^{12}\text{C}(\text{all})$, $^{13}\text{C}(1)$, $^{13}\text{C}(2)$, $^{13}\text{C}(3)$ and $^{13}\text{C}(4)$

Mode	$^{12}\text{C}(\text{all})$	$^{13}\text{C}(1)$	$^{13}\text{C}(2)$	$^{13}\text{C}(3)$	$^{13}\text{C}(4)$
26					
27					

Taking into account mean deviations and maximum deviations for all four ^{13}C species with respect to frequency and intensity it is notable that substitution in *ortho*- and *meta*-position induces the smallest frequency shifts (mean deviation: 3.6 cm^{-1} , maximum deviation: -11.7 and -10.1 cm^{-1}) but the most prominent intensity changes (mean deviation: $+73\%$ and $+26\%$, maximum deviation: 944% and 443%). This result is in particular interesting since these positions show the double probability for ^{13}C substitution than C1 and C4 based on the C_s symmetry of thiophenol. Therefore, an experimentally observed isotopic effect in highly spatial resolved Raman techniques is more likely to be verifiable by means of the alterations in the intensity pattern than by the frequencies, while certainly alterations in the intensity pattern are highly correlated to variations in the band positions due to line broadening.

4 Conclusions

In high-resolution vibrational spectroscopic techniques only a small number of molecules is in the focus of the Laser, e.g. in SERS. Thus, isotopic effects might be of enhanced importance for such techniques compared to low-resolution techniques, where a macroscopic average Raman signal is measured. In order to evaluate the magnitude of isotopic effects originating from ^{13}C (natural isotope redundancy: 98.93% ^{12}C and 1.07% ^{13}C) on both the vibrational frequencies as well as on the Raman intensities, quantum chemical calculations have been performed for the thiophenol molecule. DFT calculations using the B3LYP XC functional and the 6-31G(d) basis set yielded the fully optimized equilibrium structure of thiophenol (C_s symmetry). Subsequently, a vibrational analysis using the most abundant isotopes that is ^1H , ^{12}C and ^{32}S has been performed. Frequency calculations for the singly ^{13}C doped species in the positions C1, C2, C3 and C4 yielded the respective Raman spectra. Summation over weighted Raman spectra for the ^{12}C and the four singly ^{13}C doped species, yielded the natural redundancy Raman signal, which was found to be

almost identical to the ^{12}C reference spectrum. Hence, unsurprisingly, isotopic effects originating from ^{13}C are of marginal importance on a macroscopic scale. However, a considerable effect can be estimated with respect to high-resolution techniques. Since ^{13}C doping leads to an increased reduced mass, exclusively bathochromic shifts of the vibrational frequencies are estimated, which is confirmed by the calculations. The largest mean deviation of -6.7 cm^{-1} has been determined for the $^{13}\text{C}_4$ species, while substitution in C1, C2 and C3 leads to similar shifts of -4.0 and -3.6 cm^{-1} . The individual frequency shift of each vibrational mode was found to be strictly correlated to the displacement of the ^{13}C atom. Besides variations in the frequencies upon ^{13}C substitution, also effects with respect to the Raman intensity have been investigated. Since the Stokes intensity is proportional to $(\omega_L - \omega_I)^4$, a general increase of the intensity is estimated based on the observed bathochromic shifts. This was confirmed by the mean intensity deviations with respect to the ^{12}C reference system, where besides for $^{13}\text{C}_1$ only positive amplifications of 73% ($^{13}\text{C}_2$), 26% ($^{13}\text{C}_3$) and 11% ($^{13}\text{C}_4$) are computed. However, also intensity decrease was found for several normal modes, this is partially accounted for by mixing of normal modes upon ^{13}C substitution, which hinders a direct comparison of the specific normal modes.

The estimated influence of isotopic effects on the Raman spectrum of thiophenol can be expected to be of significant importance for single molecule detection, but also for small ensembles where due to the small numbers averaging effects cannot be expected. In both cases the isotopes will induce variations with respect to intensity and frequency.

References

1. Kneipp K, Wang Y, Kneipp H, Perelman L T, Itzkan I, Dasari R, Feld M S, *Phys Rev Lett*, 78(1997)1667-1670.
2. Ru E C Le, Meyer M, Etchegoin P G, *J Phys Chem B*, 110(2006)1944-1948.
3. Moyer P J, Schmidt J, Eng L M, Meixner A J, *J Am Chem Soc*, 122(2000)5409-5410.
4. Nie S M, Emery S R, *Science*, 275(1997)1102-1106.
5. Anderson M S, *Appl Phys Lett*, 76 (2000)3130-3132.
6. Hayazawa N, Inouye Y, Sekkat Z, Kawata S, *Opt Commun*, 183(2000)333-336.
7. Stockle R M, Suh Y D, Deckert V, Zenobi R, *Chem Phys Lett*, 318(2000)131-136.
8. Tripathi A, Emmons E D, Christesen S D, Fountain III A W, Guicheteau J A, *J Phys Chem C*, 117(2013)22834-22842.
9. Jung H Y, Park Y.-K, Park S, Kim S K, *Anal Chim Acta*, 602(2007)236-243.
10. Taylor C E, Pemberton J E, Goodman G G, Schoenfish M H, *Appl Spectrosc*, 53(1999)1212-1221.
11. Huang Y.-F, Wu D.-Y, Zhu H.-P, Zhao L.-B, Liu G.-K, Ren B, Tian Z.-Q, *Phys Chem Chem Phys*, 14(2012)8485-8497.
12. Biggs K B, Camden J P, Anker J N, Van Duyne R P, *J Phys Chem A*, 113(2009)4581-4586.
13. Smirnov V V, Lanci M P, Roth J P, *J Phys Chem A*, 113(2009)1934-1945.
14. Wiest O, Black K A, Houk K N, *J Am Chem Soc*, 116(1994)10336-10337.
15. Nicholson K M, Sholl D S, *Phys Rev B*, 86(2012)134113; doi.org/10.1103/PhysRevB.86.134113
16. Hu W P, Truhlar D G, *J Am Chem Soc*, 118(1996)860-869.
17. Pabis A, Paluch P, Szala J, Paneth P, *J Chem Theory Comput*, 5(2009)33-36.
18. Tsai W.-C, Hu W.-P, *Molecules*, 18(2013)4816-4843.
19. Villano S M, Kato S, Bierbaum V M, *J Am Chem Soc*, 128(2006)736-737.
20. Ashley D C, Brinkley D W, Roth J P, *Inorg Chem*, 49(2010)3661-3675.
21. Basova T V, Kiselev V G, Schuster B.-E, Peisert H, Chassé T, *J Raman Spectrosc*, 40(2009)2080-2087.
22. Leybold C F, Reiher M, Brehm G, Schmitt M O, Schneider S, Matousek P, Towrie M, *Phys Chem Chem Phys*, 5 (2003)1149-1157.
23. Singh D, Ojha A K, Kiefer W, Singh R K, *Vib Spectrosc*, 49(2009)242-250.

24. Palfi V K, Guillon T, Paulsen H, Molnar G, Bousseksou A, *CR Chim*, 8(2005)1317-1325.
25. Alparone A, *J Chem*, 2013(2013).
26. Frisch M J , Trucks G W, Schlegel H B, Scuseria G E, Robb M A, Cheeseman J R, Scalmani G, Barone V, Mennucci B, Petersson G A, Nakatsuji H, Caricato M, Li X, Hratchian H P, Izmaylov A F, Bloino J, Zheng G, Sonnenberg J L, Hada M, Ehara M, Toyota K, Fukuda R, Hasegawa J, Ishida M, Nakajima T, Honda Y, Kitao O, Nakai H, Vreven T, Montgomery J A (Jr), Peralta J E, Ogliaro F, Bearpark M, Heyd J J, Brothers E, Kudin K N, Staroverov V N, Kobayashi R, Normand J, Raghavachari K, Rendell A, Burant J C, Iyengar S S, Tomasi J, Cossi M, Rega N, Millam J M, Klene M, Knox J E, Cross J B, Bakken V, Adamo C, Jaramillo J, Gomperts R, Stratmann R E, Yazyev O, Austin A J, Cammi R, Pomelli C, Ochterski J W, Martin R L, Morokuma K, Zakrzewski V G, Voth G A, Salvador P, Dannenberg J J, Dapprich S, Daniels A D, Farkas O, Foresman J B, Ortiz J V, Cioslowski J, Fox D J, Gaussian 09 Revision A.02.
27. Becke A D, *J Chem Phys*, 98(1993)5648-5652.
28. Lee C, Yang W, Parr R G, *Phys Rev B*, 37(1988)785-789.
29. Hariharan P C, Pople J A, *Theor Chim Acta*, 28(1973)213-222.
30. Audi G, Wapstra A H, *Nucl Phys A*, 565(1993)1-65.
31. Audi G, Wapstra A H, *Nucl Phys A*, 595(1995)409-480.
32. Vocke R D, *Pure Appl Chem*, 71(1999)1593-1607.

[Received : 30.09.2015; accepted: 1.11.2015]

Volker Deckert is Professor at the Institute of Physical Chemistry at the Friedrich-Schiller University Jena and also heads the Nanoscopy department at the Leibniz Institute of Photonic Technologies, Jena. He received his Ph.D. from the University of Würzburg, working on Raman spectroscopy. As a post-doc his research focus shifted towards non-linear and time-resolved laser spectroscopy at the University of Tokyo and KAST, in Kawasaki. Since his habilitation at the ETH Zurich, he does research on near-field optical spectroscopy, a subject he still pursues and currently applies to biological samples and to the investigation of chemical reactivity on the nanometer scale.



Stefanie Gräfe joined the Friedrich Schiller University Jena in 2013 and is the head of the Theoretical Chemistry group at the Institute for Physical Chemistry. She has received her Ph D from the University of Würzburg working on femtosecond time-resolved quantum dynamics. As a postdoc at the Steacie Institute for Molecular Sciences of the National Research Council in Ottawa, Canada, and afterwards, at the Institute for Theoretical Physics at the Vienna University of Technology she has been working on simulating electronic dynamics in strong-field and attosecond atomic and molecular processes. Since moving to Jena, she also turned her attention to electronic processes in weaker fields, allowing with the help of quantum chemical methods to calculate ground and excited state spectroscopic properties of molecules.

